

Noise model of the cryogenic nuclear magnetic resonance spectroscopy system's receiving chain

Kolar, Petar; Blažok, Lovro; Bojanjac, Dario

Source / Izvornik: **Automatika, 2022, 63, 474 - 481**

Journal article, Published version

Rad u časopisu, Objavljena verzija rada (izdavačev PDF)

<https://doi.org/10.1080/00051144.2022.2052649>

Permanent link / Trajna poveznica: <https://urn.nsk.hr/urn:nbn:hr:217:835277>

Rights / Prava: [Attribution 4.0 International](#)/[Imenovanje 4.0 međunarodna](#)

Download date / Datum preuzimanja: **2024-11-19**



Repository / Repozitorij:

[Repository of the Faculty of Science - University of Zagreb](#)





Noise model of the cryogenic nuclear magnetic resonance spectroscopy system's receiving chain

Petar Kolar ^{a,b}, Lovro Blažok ^c and Dario Bojanjac ^a

^aFaculty of Electrical Engineering and Computing, University of Zagreb, Zagreb, Croatia; ^bFaculty of Science, Department of Physics, University of Zagreb, Zagreb, Croatia; ^cFaculty of Mining, Geology and Petroleum Engineering, University of Zagreb, Zagreb, Croatia

ABSTRACT

One of the challenges in modern nuclear magnetic resonance (NMR) is achieving its highest possible measuring sensitivity. This is because modern NMR samples' response signals decrease, so background noise of the used NMR spectroscopy system causes bigger problems. As a solution, both software and hardware interventions were applied. However, these improvements were obtained experimentally, so the reason for their proper operation and upper limit is usually unknown. Recently, a noise model of the NMR spectroscopy system, which shows both the reason for proper operation and the upper limit of the applied improvements, was introduced. A Javascript-based calculator, based on the introduced model, has been developed and made available online as a user-friendly website that can be run on the most commonly used Internet browsers. To the authors' knowledge, this calculator is the first of its kind that analyses noise properties in NMR. Using it, one can *a priori* make both sensitivity prediction of practical NMR systems in physics and material science and quantitative analysis of its noise properties. Consequently, overall measurement duration can be shortened down to one half of the current duration. This is an immense improvement, as some modern NMR measurements consume more than ten hours per measurement.

ARTICLE HISTORY

Received 23 June 2020
Accepted 7 March 2022

KEYWORDS

NMR spectroscopy; noise figure; model; sensitivity enhancement; Python; Javascript

1. Introduction

The aim of this article is to present the newly-developed noise figure calculator intended to be used in the condensed matter physics nuclear magnetic resonance (NMR) spectroscopy systems. To the authors' knowledge, this calculator is the first calculator of its kind that can *a priori* predict noise properties of the NMR spectroscopy systems. However, before the introduction of the calculator itself, which is presented in Sections 3 and 4 of this article, the authors wish to familiarise the reader with the NMR spectroscopy systems' mode of operation (Section 1), as well as with the main problems of modern NMR measurements (Section 2).

Nuclear magnetic resonance (NMR) is a physical phenomenon that is used to study materials via the interaction between the radio frequency (RF) electromagnetic (EM) radiation and the observed material's nuclei placed in a strong magnetic field. This phenomenon is analogous to the process of stimulated emission in lasers: while the population inversion of electrons causes the emission of photons (which is the EM field in the optical frequency range between around 400 THz and around 800 THz) in lasers [1], the population inversion of magnetic spins causes the emission of EM field in the High Frequency (HF), Very High

Frequency (VHF) or Ultra High Frequency (UHF) band in NMR [2,3]. Furthermore, NMR spectroscopy is a spectroscopic technique, based on the phenomenon of NMR, that is used to observe local magnetic fields around atomic nuclei [4] and thus determine the chemical and physical properties of the atoms or molecules these atoms are placed in.

The basic diagram of the cryogenic NMR spectroscopy system, used in condensed matter physics, can be seen in Figure 1. This system has two modes of operation: the transmitting (Tx) mode and the receiving (Rx) mode. During the Tx mode, high-power pulses (up to the order of a kW) are generated by a signal generator inside the spectrometer (this instrument will soon prove to be the main part of this NMR spectroscopy system) in order to excite the sample's nuclei. These pulses are then amplified by a power amplifier and transmitted to the probe's coil via the duplexer. There, they generate a magnetic field that excites the nuclei of the sample under measurement. This is the end of the Tx mode and the system "switches" to the Rx mode. The response signal of the sample has a very low magnitude (sometimes even down to the order of an fW), so it needs to be amplified before arriving at the spectrometer's receiver. This amplification is achieved

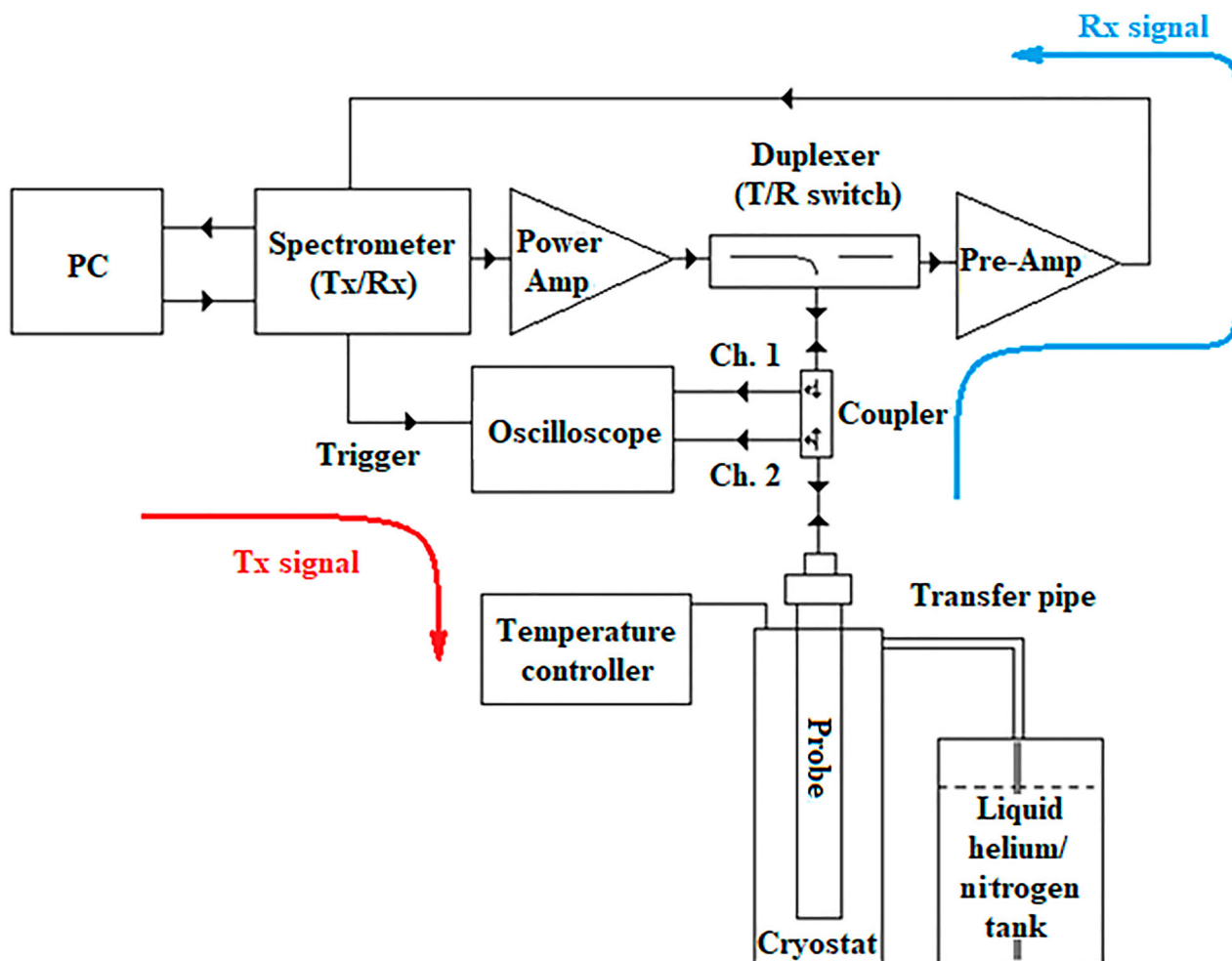


Figure 1. Basic schematic diagram of the cryogenic NMR spectroscopy system used in condensed matter physics [5].

by a low-noise NMR preamplifier. In the spectrometer, the received signal is firstly down-converted to an intermediate frequency and then further amplified by a variable-gain amplifier, which allows amplitude optimization before analogue-to-digital (A/D) conversion. After the detection and A/D conversion, the signal gets post-processed digitally, using different methods, such as time averaging of multiple measurement results and digital filtering. Finally, such a signal is then displayed on the spectrometer screen [6,7].

At first glance, this system might seem a bit exotic and difficult to understand. So, to completely demystify this system to every reader of this article, a much more commonly popular system will be mentioned, and that system is – Magnetic Resonance Imaging (MRI)! This system is used in hospitals in order to form pictures of the physiological processes and the anatomy of the human body. But this system is just a special case of NMR spectroscopy, where hydrogen atoms of water molecules inside the human body are measured [8].

2. The problematics of modern NMR measurements

The reason the human body is measured with MRI by measuring hydrogen atoms in water molecules is

because, first of all, the human body is comprised of 70% water, and second of all, hydrogen has a very high NMR (because, again, MRI is just a special case of NMR spectroscopy) response signal. This is why MRI scans are of such high quality and resolution. However, not all chemical elements have such a good response signal. In fact, many modern NMR measurements are purposely performed on the atoms or molecules that have very low response signals, so that some relatively new and currently popular phenomena, like, for example, superconductivity [9–12], could be analysed. Due to the fact that modern NMR samples have response signals of very low levels, the background noise of the NMR spectroscopy system became a serious problem. In fact, the levels of response signals very often achieve values lower than the values of the system's background noise. To fix this problem, the most commonly used solution is the time averaging of multiple measurement results. This is a pretty powerful tool for tackling the background noise problem; however, the response signal levels of some modern NMR samples are so low, that the averaging starts consuming exhausting amounts of time. For example, the measurements of some samples, including the averaging, can even last longer than 10 hours for a single dataset [13]! In order to reduce the background noise of the NMR spectroscopy system,

and thus reduce the number of measurement results to be averaged (therefore, to shorten the overall measurement time), some hardware interventions, like cryogenical cooling of the NMR probe or its coil [14] and the NMR preamplifier [15] were applied to the system of NMR spectroscopy. However, these improvements were achieved experimentally, that is, by repeating the same experiment with different system parameters until satisfactory parameters were obtained. Therefore, the limitations and maximum possible improvements of the used NMR spectroscopy systems usually remain unknown.

3. NMR spectroscopy system receiving chain's noise figure model

Recently [6], a noise model, based on the concept of noise figure [16,17], of the most sensitive part of the NMR spectroscopy system from the aspect of noise, which is its receiving (Rx) chain, has been introduced. It is based on the concept of noise figure because, with its usage, it is relatively easy to calculate the overall noise figure of the cascade (which the Rx chain of the described system really is) and also because power gains and power losses of every single element of the chain can either be easily measured with the usage of vector network analysers (VNAs) [18] or are available in the datasheet of the respective element. Furthermore, noise figures of every element are also available in the datasheet of the respective element or can be measured with the help of noise figure (NF) metres [19], except the one of the spectrometer, which can be determined with the usage of the so-called "Twice Power Method" [5,20].

$$F_{NMR_{Rx}} = \frac{1 + \frac{2T_0}{T_{coil} + T_0} \left[L_1 + L_1(L_2 - 1) + \frac{L_1 L_2 (F_3 - 1)}{1 - |S_{113}|^2} + \frac{L_1 L_2 (L_4 - 1)}{G_3 (1 - |S_{113}|^2)} + \frac{L_1 L_2 L_4 (F_5 - 1)}{G_3 (1 - |S_{113}|^2)} - 1 \right]}{n_{meas}} \quad (1)$$

$$F_{NMR_{Rx}} = \frac{1}{n_{meas}} + \frac{2T_0}{T_{coil} + T_0} \cdot \frac{\left[L_1 + L_1(L_2 - 1) + \frac{L_1 L_2 (F_3 - 1)}{1 - |S_{113}|^2} \right]}{n_{meas}} + \frac{2T_0}{T_{coil} + T_0} \cdot \frac{\left[\frac{L_1 L_2 (F_3 - 1)}{G_3 (1 - |S_{113}|^2) (1 - |S_{113b}|^2)} + \frac{L_1 L_2 (L_4 - 1)}{G_3 (1 - |S_{113}|^2) G_{3b} (1 - |S_{113b}|^2)} \right]}{n_{meas}} + \frac{2T_0}{T_{coil} + T_0} \cdot \frac{\left[\frac{L_1 L_2 L_4 (F_5 - 1)}{G_3 (1 - |S_{113}|^2) G_{3b} (1 - |S_{113b}|^2)} - 1 \right]}{n_{meas}} \quad (2)$$

The block diagram of the developed model can be seen in Figures 2 and 3, while the expressions that describe the developed model can be seen below the respective figures, in (1) and (2). To the authors' knowledge, this is the first numerical model of the NMR spectroscopy system that explains why and how the applied enhancements to the NMR spectroscopy system (averaging, cryogenical cooling) work. Also, it is important to stress that the aforementioned model was developed using a multidisciplinary approach that combines the knowledge of microwave and RF engineering with the knowledge of solid state and condensed matter physics. Therefore, the described development of the introduced model supports the hypothesis which states that multidisciplinary studies are the future of science in general [21]. The most important discovery that the introduced model shows are the breaking of the myth which states that acquiring an NMR preamplifier with extremely low-noise figure will solve the NMR spectroscopy system's background noise problem itself. While having an NMR preamplifier with its noise figure as low as possible does come in handy, this is actually priority number two. Priority number one, as the introduced model has shown, is having an NMR preamplifier with the absolute value of its power gain level higher than the absolute value of the spectrometer's noise figure. Having such a preamplifier, the spectrometer's high-level noise figure value (compared to the noise figure values of the rest of the elements in the Rx chain) gets suppressed. As it was shown in [5,6] that the spectrometer is undoubtedly the greatest contributor to the background noise of the entire system, suppressing the noise value that it injects into the system decreases the overall noise figure of the system substantially, and thus, the overall measurement time is shortened!

4. The usage of the introduced model

Before performing the actual NMR measurement, first, it is necessary to determine the right system parameters of the used NMR spectroscopy system (the right number of measurements, the applicable tuning of the probe, the appropriate chain elements of the Rx chain...). This is done by performing multiple measurements with different sets of system parameters, until the satisfactory set of parameters is found (this is the so-called *a posteriori* approach) [6]. If the duration of a single measurement lasts a few minutes or maybe an hour, this is obviously not a problem. However, if a single measurement lasts more than 10 hours (as it is the case with [13]), then one needs to spend a huge amount of time just to prepare the system for the actual NMR measurement! So instead of performing these preparatory measurements, the idea is to use the introduced noise model of the NMR spectroscopy system Rx chain in order to determine the optimal parameters (this is

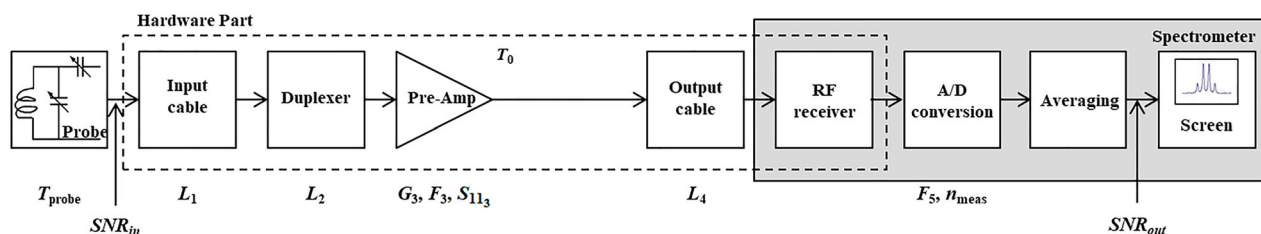


Figure 2. Block diagram of the NMR spectroscopy receiving chain with a single-stage preamplifier [5] (up) and its noise figure expression (down) [6].

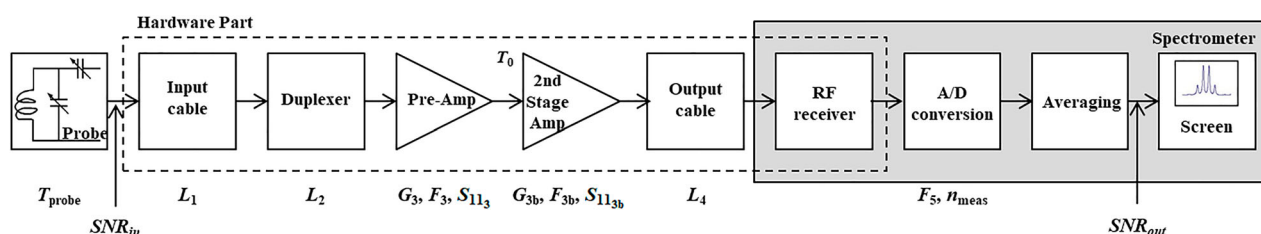


Figure 3. Block diagram of the NMR spectroscopy receiving chain with a two-stage preamplifier [5] (up) and its noise figure expression (down) [6].

the so-called *a priori* approach). Like so, the preparation of the system would take none or one preparatory measurement, which clearly consumes notably less time than the *a posteriori* approach [5].

Nonetheless, as it can be seen, the expressions (1) and (2) are somewhat lengthy and using them manually is a very error-prone process. That is why these two expressions have been "moulded" into a Python-written program that calculates noise figure of the NMR spectroscopy Rx chain and appropriate input and output signal-to-noise ratios. The used version of Python is 3.6 (32-bit). This program is made available online via GitHub [23] or Dropbox [24]. Furthermore, as not everybody uses Python and its integrated development environment, a new, Javascript-based program has been developed. This program has been made available online in a form of a user-friendly calculator based on the aforementioned model [22]. The list of input parameters used in the calculator can be seen in Tables 1 and 2. This way, anyone can use this program without the need to install additional development environments. Also, the minimalistic design and the user-friendly data input should ensure a simple and intuitive use of the developed calculator. A few screenshots of the calculator during its usage can be seen in Figures 4 and 5.

Except for the primary reason to use this calculator, which is the *a priori* determination of the appropriate NMR spectroscopy system parameters, as well as the estimation of the NMR measurement result before actually performing the measurement itself, the authors feel that this calculator could also be used for educational purposes. Namely, in the academic courses where NMR spectroscopy is taught, like solid-state physics and condensed matter physics courses, the proposed model can be used to explain the pros and cons

Table 1. A list of input parameters that are used in NMR-Calc [22].

Label	Explanation
T_{probe}	Coil temperature in K
SNR_{in}	Input power signal-to-noise ratio in dB
L_1	Input cable power loss in dB
L_2	Duplexer power loss in dB
G_3	NMR preamplifier power gain in dB
F_3	NMR preamplifier noise figure in dB
S_{113}	NMR preamplifier input reflection coefficient in dB
G_{3b}	2nd stage amplifier power gain in dB
F_{3b}	2nd stage amplifier noise figure in dB
S_{113b}	2nd stage amplifier input reflection coefficient in dB
L_4	Output cable power loss in dB
F_5	Spectrometer noise figure in dB
n_{meas}	Number of averaged measurements
SNR_{out}	Output power signal-to-noise ratio in dB

Table 2. A list of used input parameters for every specific model available in NMRCalc [22].

Parameter	Model (M) and Path (P)			
	M1 P1	M1 P2	M2 P1	M2 P2
T_{probe}	✓	✓	✓	✓
SNR_{in}	✓		✓	
L_1	✓	✓	✓	✓
L_2	✓	✓	✓	✓
G_3	✓	✓	✓	✓
F_3	✓	✓	✓	✓
S_{113}	✓	✓	✓	✓
G_{3b}			✓	✓
F_{3b}			✓	✓
S_{113b}			✓	✓
L_4	✓	✓	✓	✓
F_5	✓	✓	✓	✓
n_{meas}	✓	✓	✓	✓
SNR_{out}		✓		✓

of having a good (or bad) NMR measurement setup, observed from the aspect of the system's background noise properties. The lecturer could, for example, input ideal system parameters (which are too good to be true)

Model 2

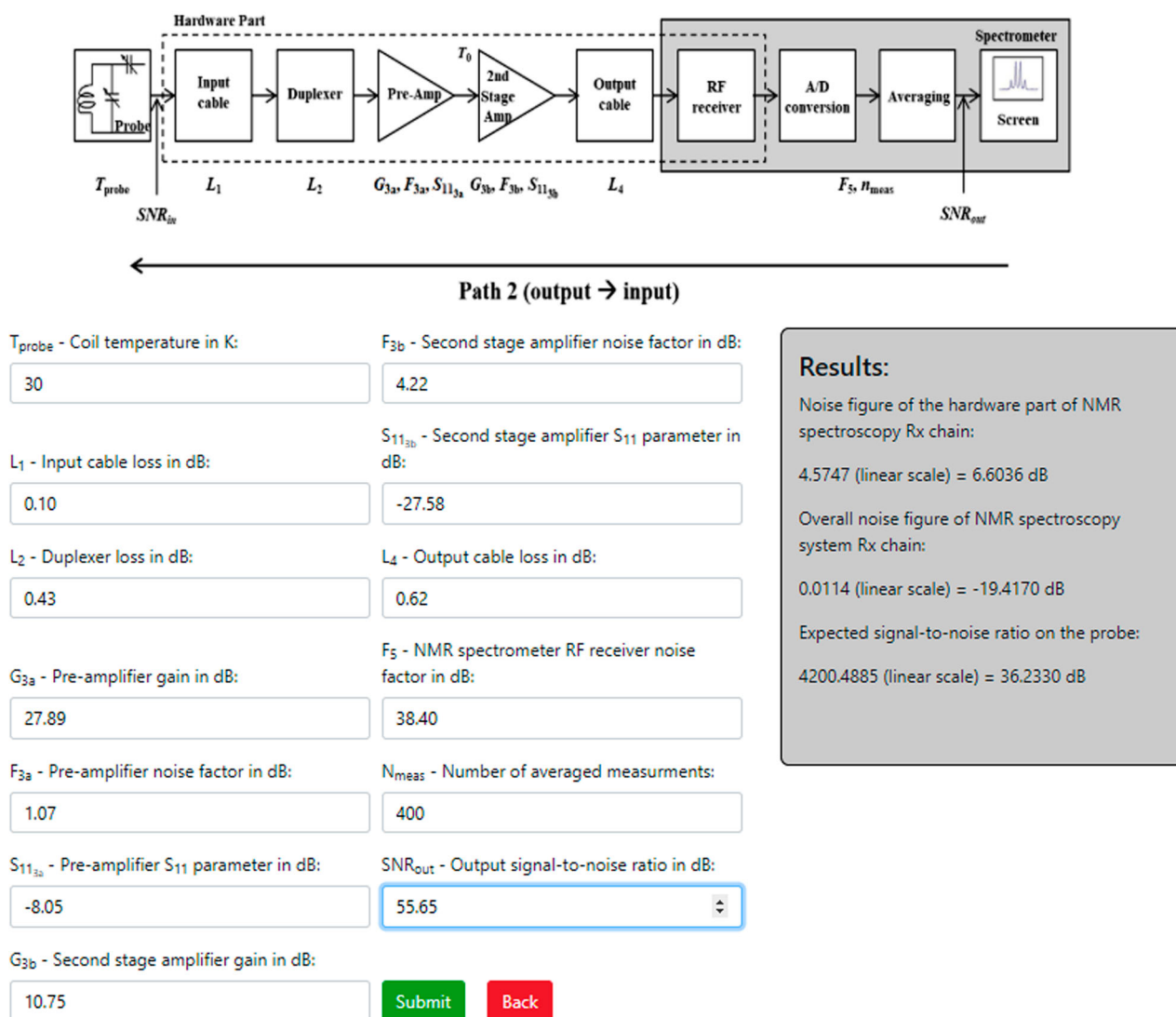


Figure 4. The screenshot of the NMRCalc [22,27] usage to perform the ^{133}Cs in $\text{Cs}_2\text{Cu}_3\text{SnF}_{12}$ measurement [6] prediction using the model M2 P2. For an image with better resolution, check the actual calculator [22].

into the model and show the students the theoretical limits of the used NMR spectroscopy system. Or, on the other hand, one could purposely input parameters that are quite the opposite of the ideal situation and then observe the deterioration of the signal quality throughout the entire NMR spectroscopy Rx chain, as well as the influence of every Rx chain's element on the system's overall background noise level. This way, the developed model would not only decrease the overall preparation time of the NMR spectroscopy system setup and the overall NMR measurement time, it also has the potential to increase the knowledge and strengthen the understanding of the importance of having an optimal NMR spectroscopy system setup, as well as the noise level decreasing techniques, which are used to guide the NMR spectroscopy system parameters to the optimal values. The latter would not only be true for the students that have just started learning the NMR spectroscopy system but also for their professors, as the developed model [6] was introduced only recently.

5. Testing the introduced calculator

In order to test the precision and the correctness of the introduced calculator, NMRCalc, the measurement results presented in [6] and the parameters of the NMR spectroscopy system used to obtain the aforementioned results were input into NMRCalc. The idea was to compare the prediction results obtained in [6] with the prediction results obtained using NMRCalc. In the end, two comparisons were made. The first one was the comparison of the ^{133}Cs in $\text{Cs}_2\text{Cu}_3\text{SnF}_{12}$ measurement, presented in the far right columns of Tables 1 and 3 in [6] (three measurements with three different setups), while the second one was the comparison of the ^{63}Cu in SeCuO_3 measurement, presented in the middle columns of Tables 1 and 4 in [6] (two measurements with two different setups). So, five different measurements were made in order to test and confirm the repeatability of the calculator in a similar way to the scientific work presented in [25,26]. The only difference

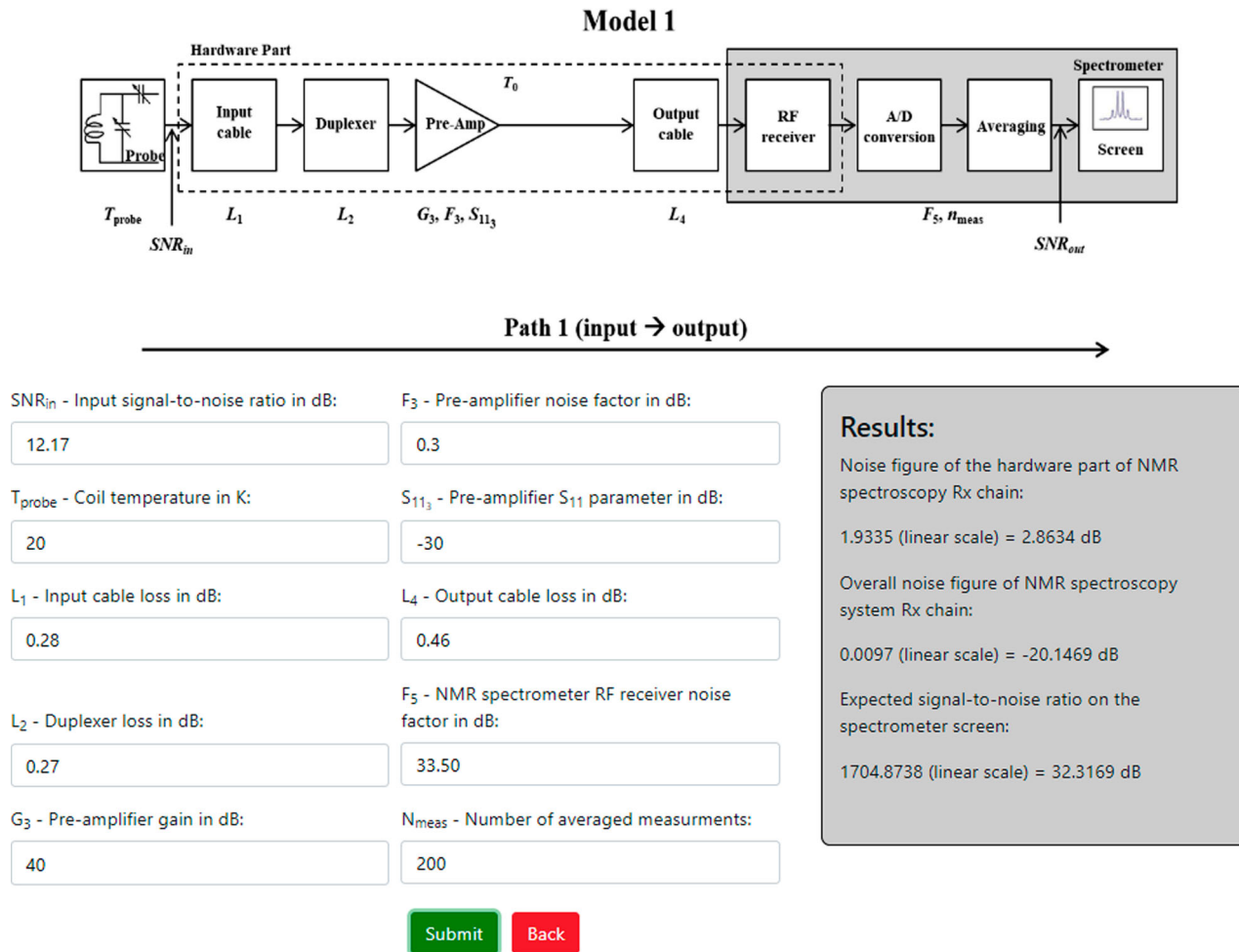


Figure 5. The screenshot of the NMRCalc [22,27] usage to perform the ^{63}Cu in SeCuO_3 measurement [6] prediction using the model M1 P1. For an image with better resolution, check the actual calculator [22].

is that [25,26] measure complex biological fluids at temperatures around room temperature, while here, solid alloys were measured at temperatures around absolute zero (the measured samples were immersed in liquid nitrogen and liquid helium). This way, models M2 P2 and M1 P1 (presented in Table 2), respectively, were tested. The screenshots of NMRCalc usage to make predictions for the ^{133}Cs in $\text{Cs}_2\text{Cu}_3\text{SnF}_{12}$ measurement and the ^{63}Cu in SeCuO_3 measurement can be seen in Figures 4 and 5, respectively. As it can be seen in Figure 4, the expected signal-to-noise ratio (SNR) on the probe, obtained using NMRCalc, is equal to 36.23 dB, while the same value, presented in [6], is equal to 36.24 dB. The difference of 0.01 dB between the two values is equal to the error of 0.23% in the power scale, which is within the limit of a rounding error. Furthermore, as it can be seen in Figure 5, the expected SNR on the spectrometer screen, obtained using NMRCalc, is equal to 32.32 dB, while the same value, presented in [6], is equal to 32.28 dB. Here, the difference of 0.04 dB between the two values is equal to the error of 0.93% in the power scale, which is, again, within the limit of a rounding error. Therefore, the consistency of the comparison results proves the precision and the correctness of the introduced calculator, NMRCalc.

6. The global availability of the introduced model

The calculator website operation has been tested on multiple Internet browsers, and the list of Internet browsers and their versions, where the developed calculator can be used, is available in Table 3. As it can be seen in Table 3, there is a wide variety of Internet browsers, which currently cover almost 90% of the Internet browser market share worldwide (according to [28]), that can be used to run the developed calculator based on the proposed model. The browsers included are the preset browsers for modern Microsoft and Apple operating systems, as well as most Linux operating systems. Therefore, the proposed model is made available worldwide, and it does not require any additional necessary instalments and usages of different browsers or some other software.

Furthermore, a YouTube channel, whose intended purpose is to support the developed calculator, NMRCalc [22], has been created. This channel is enlisted in the References of this article under [29]. Currently, there are two videos uploaded to the aforementioned channel: the first video explains the motivation on why to use NMRCalc in the first place, while the second

Table 3. A list of tested Internet browsers that can be used to run the website with the developed calculator, NMRCalc [22]

Internet Browser	Version
Google Chrome	80.0.3987.149 64-bit
Microsoft Edge	80.0.361.69 64-bit
Chromium	83.0.4099.0 64-bit
Mozilla Firefox	74.0 64-bit
Opera	67.0.3575.115 64-bit
Safari	13.1 (15609.1.20.111.8) 64-bit

video contains a detailed description of how to properly use NMRCalc. The description is performed through a simple yet realistic practical example, which occurs quite often when using a real-life NMR spectroscopy system. This way, the potential new user obtains the full impression of NMRCalc and its features straight away.

Again, the authors wish to point out that, to their knowledge, NMRCalc is the first calculator of its kind that analyses noise properties of condensed matter physics NMR spectroscopy systems, which is exactly the reason why the calculator has been created and made available online. Therefore, it is hard for the authors to talk about similar solutions, as they are unaware of such, if they are even available.

7. Conclusion

The introduced noise figure-based model of the NMR spectroscopy system showed that, while having an NMR preamplifier with an extremely low-noise figure does come in handy, having an NMR preamplifier with its absolute power gain higher than the absolute value of the spectrometer's noise figure is much more important in order to achieve the highest possible measuring sensitivity of the used NMR spectroscopy system. The developed model not only has the potential to decrease the overall preparation time of the system setup and the overall NMR measurement time but also has the potential to increase the knowledge and strengthen the understanding of the importance of having an optimal NMR spectroscopy system setup, as well as noise level decreasing techniques, which are used to guide the system parameters to their optimal values. The latter would not only be true for the students that have just started learning the NMR spectroscopy system but also for their professors, as the developed model was introduced only recently. A Javascript-based calculator of the introduced model, whose purpose is to calculate noise figure of the NMR spectroscopy Rx chain and to predict SNR value either at the input or at the output of the aforementioned chain, has been developed and made available online. By using this calculator, the user can save both time (as the calculator showed that overall NMR measurements' duration could be cut down to one half of its current duration) and money (as the calculator showed that buying expensive electronic equipment does not necessarily improve the

NMR spectroscopy system's overall noise properties and overall sensitivity). This calculator is used as a user-friendly website that can be run on multiple Internet browsers, which currently cover almost 90 % of their market share worldwide. To the authors' knowledge, such a calculator is the first available NMR calculator of this kind.

Disclosure statement

No potential conflict of interest was reported by the author(s).

ORCID

Petar Kolar  <http://orcid.org/0000-0001-9263-7946>

Lovro Blažok  <http://orcid.org/0000-0002-4210-6925>

Dario Bojanjac  <http://orcid.org/0000-0001-9969-1849>

References

- [1] Silfvast WT. *Laser fundamentals*. 2nd ed. Cambridge: Cambridge University Press; 2008.
- [2] Abragam A. *The principles of nuclear magnetism*. Oxford: Oxford University Press; 1978.
- [3] Slichter CP. *Principles of magnetic resonance*. 3rd ed. Berlin: Springer-Verlag; 1990.
- [4] Rahman A, Choudhary M, Wahab A. *Solving problems with NMR spectroscopy*. 2nd ed. San Diego (CA): Elsevier Academic Press; 2016.
- [5] Kolar P. *Optimization of radio frequency components of cryogenic Nuclear Magnetic Resonance spectroscopy system [dissertation]*. Zagreb, Croatia: University of Zagreb; 2020 Feb.
- [6] Kolar P, Grbić MS, Hrabar S. Sensitivity enhancement of NMR spectroscopy receiving chain used in condensed matter physics. *Sensors*. 2019 Jul;19(14):3064.
- [7] Krauss HL, Bostian CW, Raab FH. *Solid state radio engineering*. New York (NY): Wiley; 1980.
- [8] Dale BM, Brown MA, Semelka RC. *MRI: basic principles and applications*. 5th ed. Chichester: Wiley Blackwell; 2015.
- [9] Freitas JCC, Scopel WL, Paz WS, et al. Determination of the hyperfine magnetic field in magnetic carbon-based materials: DFT calculations and NMR experiments. *Sci Rep*. 2015 Oct;5:14761.
- [10] Blinder R, Dupont M, Mukhopadhyay S, et al. Nuclear magnetic resonance study of the magnetic-field-induced ordered phase in the $\text{NiCl}_2\text{-4SC(NH}_2)_2$ compound. *Phys Rev B*. 2017 Jan;95:020404 (R).
- [11] Pelc D, Grafe HJ, Gu GD, et al. Cu nuclear magnetic resonance study of charge and spin stripe order in $\text{La}_{1.875}\text{Ba}_{0.125}\text{CuO}_4$. *Phys Rev B*. 2017 Feb;95:054508.
- [12] Cvitanic T, Šurija V, Prša K, et al. Singlet state formation and its impact on the magnetic structure in the tetramer system SeCuO_3 . *Phys Rev B*. 2018 Aug;98:054409.
- [13] Kleckner IR, Foster MP. An introduction to NMR-based approaches for measuring protein dynamics. *Biochim Biophys Acta (BBA)*. 2011 Aug;1814(8):942–968.
- [14] Styles P, Soffe N, Scott C, et al. A high-resolution NMR probe in which the coil and preamplifier are cooled with liquid helium. *J Mag Reson*. 1984 Dec;60(3):397–404.
- [15] Richards MG, Andrews AR, Lusher CP, et al. Cryogenic GaAs FET amplifiers and their use in NMR detection. *Rev Sci Instrum*. 1986 Oct;57(3):404–409.
- [16] Motchenbacher CD, Connelly JA. *Low-noise electronic system design*. Toronto: Wiley; 1993.

- [17] Pozar DM. Microwave engineering. Hoboken (NJ): Wiley; 2012.
- [18] Hiebel M. Fundamentals of vector network analysis. 6th ed. Munich: Rohde & Schwarz; 2014.
- [19] Keysight Technologies. Fundamentals of RF and microwave noise figure measurements. Application note, 19 June 2020. [Online]. Available from: <https://www.testworld.com/wp-content/uploads/Fundamentals-of-RF-Microwave-Noise-Figure-Measurements.pdf>.
- [20] Kolar P, Blažok L, Bojanjac D. How (and why) to determine NMR spectrometer's noise figure?. *tm – Technisches Messen*. 2020 Aug;87(10):614–621.
- [21] Kline SJ. Conceptual foundations for multidisciplinary thinking. 1st ed. Stanford: Stanford University Press; 1995.
- [22] NMRCalc Team. NMRCalc: NMR Spectroscopy Rx chain noise figure calculator. Website, 19 June 2020. [Online]. Available from: <https://nmrcalc.github.io/>.
- [23] Kolar P. NMR spectroscopy Rx chain noise figure calculator. GitHub, 19 June 2020. [Online]. Available from: https://github.com/5ARK/NMR_F_Calc.
- [24] Kolar P. NMR spectroscopy Rx chain noise figure calculator. Dropbox, 19 June 2020. [Online]. Available from: https://www.dropbox.com/s/ah3fl94zxshya7q/NMR_Rx_NF_Calculator.rar?dl=0.
- [25] Napoli PE, Nioi M, Gabiati L, et al. Repeatability and reproducibility of post-mortem central corneal thickness measurements using a portable optical coherence tomography system in humans: a prospective multi-center study. *Sci Rep*. 2020 Sep;10:14508.
- [26] Napoli PE, Nioi M. The Bull's eye pattern of the tear film in humans during visual fixation on en-Face optical coherence tomography. *Sci Rep*. 2019 Feb;9:1413.
- [27] Kolar P, Blažok L, Bojanjac D. NMR spectroscopy threshold signal-to-noise ratio. *tm – Technisches Messen*. 2021 Apr;88(9):571–580.
- [28] GlobalStats. Browser market share worldwide: Jun 2019 – Jun 2020. GlobalStats statcounter website, 19 June 2020. [Online]. Available from: <https://gs.statcounter.com/browser-market-share#monthly-201906-202006-bar>.
- [29] NMRCalc Team. NMRCalc Support. YouTube channel, n.d. [Online]. Available from: <https://www.youtube.com/channel/UCxmr6qfK3Yq-3RveHQRJBKq>.